



This is a repository copy of *Validation of near-field blast loading in LS-DYNA*.

White Rose Research Online URL for this paper:

<https://eprints.whiterose.ac.uk/134828/>

Version: Accepted Version

Proceedings Paper:

Rigby, S.E., Fuller, B. and Tyas, A. (2018) Validation of near-field blast loading in LS-DYNA. In: Proceedings of the 5th International Conference on Protective Structures. 5th International Conference on Protective Structures, 20-23 Aug 2018, Poznan, Poland. International Association of Protective Structures .

© 2018 The Author(s). For reuse permissions, please contact the Author(s).

Reuse

Items deposited in White Rose Research Online are protected by copyright, with all rights reserved unless indicated otherwise. They may be downloaded and/or printed for private study, or other acts as permitted by national copyright laws. The publisher or other rights holders may allow further reproduction and re-use of the full text version. This is indicated by the licence information on the White Rose Research Online record for the item.

Takedown

If you consider content in White Rose Research Online to be in breach of UK law, please notify us by emailing eprints@whiterose.ac.uk including the URL of the record and the reason for the withdrawal request.



eprints@whiterose.ac.uk
<https://eprints.whiterose.ac.uk/>

Validation of Near-Field Blast Loading in LS-DYNA

Sam Rigby, Ben Fuller, Andy Tyas

*Department of Civil & Structural Engineering, University of Sheffield, Mappin Building, Mappin Street, Sheffield, S1 3JD, UK
sam.rigby@sheffield.ac.uk*

Abstract

The detonation of a high explosive releases a significant amount of energy over a very small timescale, resulting in the propagation of shock waves with MPa–GPa magnitudes and μs –ms durations. Whilst current numerical modelling approaches can simulate high explosive blast events through the solution of conservation laws, the scarcity of definitive, repeatable, and high-quality experimental data has prohibited any detailed validation studies from being conducted. As such, the accuracy of numerical approaches remains largely unquantified. This paper presents the results from a series of experimental trials where the reflected blast pressures from spherical and cylindrical high explosives were directly measured. These results are used to validate LS-DYNA numerical simulations. It is shown that spherical charge simulations are in excellent agreement with the experiments, however the agreement between model and experiment was poor for the cylindrical charge simulations. Despite this, the fireball expansion rate is shown to be similar between model and experiment, suggesting that qualitative validation data should be used with caution for near-field blast events.

1 Introduction

Experimental quantification of the blast load imparted to a structure following the detonation of a high explosive began in earnest around the time of World War II (see Esparza [1] for a detailed review). Until recently, however, there have been very few accounts of direct measurement of explosive effects acting on structures located extremely close to the charge (a distance of typically less than ten charge radii).

The semi-empirical predictive method of Kingery & Bulmash (KB) [2] is well established, and recent studies (e.g. [3]) have shown that KB predictions are accurate for far-field ($Z > 4 \text{ m/kg}^{1/3}$), geometrically simple scenarios. In the extreme near-field ($Z < 1 \text{ m/kg}^{1/3}$), however, the KB predictions were derived from non-direct measurements or rudimentary numerical analyses, and have been shown to differ from numerical model results by $>400\%$ [4].

There is a clear need to establish a benchmark dataset for near-field blast loading, from direct measurement of high explosive detonations, in order to critically assess the validity and accuracy of current numerical modelling approaches. This paper presents results from direct experimental measurement of the spatial and temporal distribution of loading following a high explosive detonation. Corresponding numerical analyses using LS-DYNA [5] are validated using the experimental results and conclusions are drawn relating to the accuracy of current numerical modelling approaches.

2 Experimental apparatus and test plan

Blast load distributions were measured in a series of experimental trials conducted at the University of Sheffield Blast & Impact Laboratory in Buxton, UK, using the Characterisation of Blast Loading (CoBL) apparatus [6]. The CoBL apparatus (Figure 1(a)) comprises a pair of stiff, massive, fibre and bar reinforced concrete frames spaced 1 m apart, with each frame comprising two 500 mm square columns with a 750 mm deep, 500 mm wide concrete beam spanning horizontally between the two columns. A

100 mm thick, 1400 mm diameter high-strength steel target plate is underslung from the soffits of the horizontal beams. The target plate acts as a nominally rigid boundary to reflect the shock wave and detonation products impinging on the plate.

The target plate is drilled through its thickness to allow 10 mm diameter, 3.25 m long EN24(T) steel Hopkinson Pressure bars (HPBs) [7] to be mounted and set with their loaded faces flush with the underside of the target plate. A total of 17 bars were used; one central bar and four bars located at each radial offset of 25, 50, 75 and 100 mm from the plate centre, see Figure 1(b).

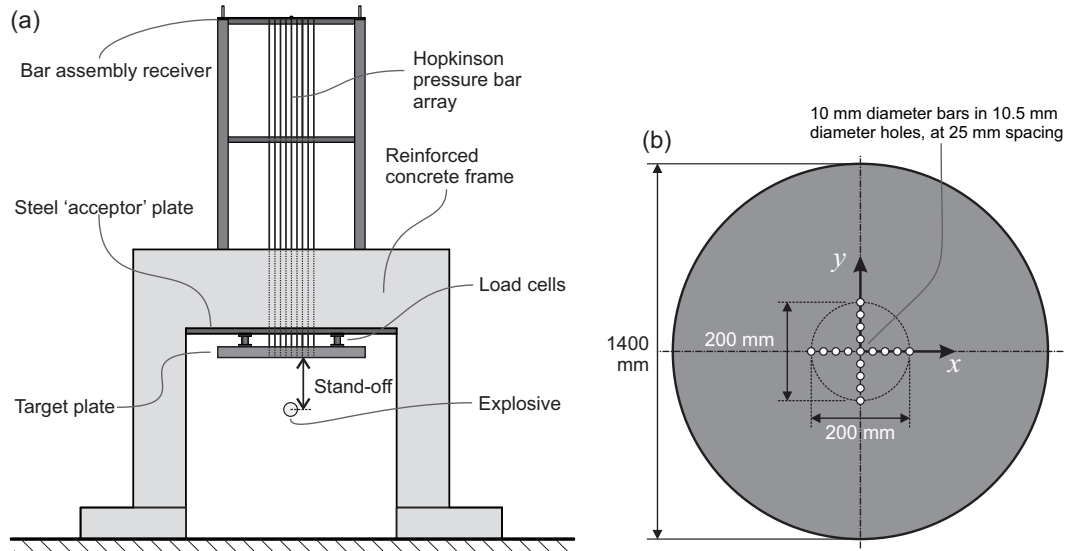


Figure 1: Schematic of testing apparatus [not to scale]: (a) elevation; (b) detailed plan view of target plate showing bar arrangement and coordinate axes (adapted from [8])

Semi-conductor strain gauges were mounted on the perimeter of each HPB, 250 mm from the loaded face, and were triggered via a voltage drop in a breakwire wrapped around the detonator. A number of tests were filmed with a Photron SA-Z high speed video (HSV) camera at 100,000 frames per second, and are used to compare experimental and numerical fireball expansion rates later in this article.

Six tests were conducted in total: three using 100 g PE4 spheres detonated at 55.4 mm clear distance to the target, and three using 78 g PE4 formed into 3:1 diameter:height cylinders, detonated at 168.0 mm clear distance to the target (Table 1). The charges in the cylinder tests, tests 4–6, were encased in 3 mm thick PVC containers with the lid removed, however additional testing showed that the casing had negligible influence on the development of load over the instrumented area [9], and hence the charge casing is ignored in subsequent numerical models.

Table 1: Test plan

Test no.	Charge mass (g PE4)	Stand-off from charge centre (mm)	Stand-off from charge surface (mm)	Charge radius (mm)	Charge height (mm)	Explosive shape
1–3	100	80.0	55.4	24.6	49.2	sphere
4–6	78	177.5	168.0	28.6	19.0	3:1 cylinder

The charges in tests 1–3 were suspended directly under the centre of the target plate on a ‘drumskin’ comprising a glass-fibre weave fabric (density 25 g/m²) held taut in a steel ring, set on adjustable struts mounted in the base of the test arena. The charges in tests 4–6 were placed on a small timber prop, sat inside an empty steel container to match the geometry of previous testing with buried explosives [8]. In all tests the charges were aligned with the plate centre using an alignment laser. The charges were detonated using Nitronel MS 25 non-electronic shock-tube detonators (700 mg PETN) inserted through the bottom face of the charge to a depth marked on the detonator corresponding to the charge radius (tests 1–3) or half charge height (tests 4–6).

3 Numerical modelling

The Multi-Material Eulerian/Arbitrary Lagrangian-Eulerian solver in LS-DYNA [5] was used to simulate the detonation process, and subsequent shock wave propagation and interaction with a rigid obstacle. The air was modelled using the *MAT_NULL material model and *EOS_LINEAR_POLYNOMIAL equation of state (EOS), given as:

$$p = C_0 + C_1\mu + C_2\mu^2 + C_3\mu^3 + (C_4 + C_5\mu + C_6\mu^2)E \quad (1)$$

where $C_0, C_1, C_2, C_3, C_4, C_5, C_6$ are constants, $\mu = \rho/\rho_0 - 1$, where ρ and ρ_0 are the current and initial densities of air respectively, and E is the specific internal energy. If the variables C_0, C_1, C_2, C_3 and C_6 are all set to equal 0, and C_4 and C_5 are set to equal $\gamma - 1$, where γ is the ratio of specific heats ($\gamma = 1.4$ for air), the ideal gas EOS is recovered:

$$p = (\gamma - 1)E\rho/\rho_0 \quad (2)$$

The initial specific internal energy was set as $E_0 = 253.4$ kPa to give an atmospheric pressure of 101.4 kPa. The explosive was modelled using the *MAT_HIGH_EXPLOSIVE_BURN material model and Jones-Wilkins-Lee (JWL) semi-empirical equation of state, *EOS_JWL [10]. The density, ρ , detonation velocity, D , and Chapman-Jouguet pressure, P_{CJ} , of the explosive are defined in the material model and control the programmed detonation of the explosive. The pressure–volume–energy relation of the explosive products post-detonation is given as:

$$p = A \left(1 - \frac{\omega}{R_1 V}\right) e^{-R_1 V} + B \left(1 - \frac{\omega}{R_2 V}\right) e^{-R_2 V} + \frac{\omega E}{V} \quad (3)$$

where A, B, R_1, R_2 and ω are constants, V is the volume and E is the specific internal energy as before. The material properties and EOS parameters for air and PE4 are given in Table 2. As PE4 is nominally identical to C4 [11], the EOS parameters for PE4 were taken as the C4 parameters published by Dobratz & Crawford [12].

Table 2: Material model and equation of state parameters for air and PE4 [12]

*MAT_NULL			*MAT_HIGH_EXPLOSIVE_BURN		
Parameter	Value	Unit	Parameter	Value	Unit
ρ_0	1.225	kg/m ³	ρ_0	1601	kg/m ³
			D	8193	m/s
			P_{CJ}	28.00E9	Pa
*EOS_LINEAR_POLYNOMIAL			*EOS_JWL		
Parameter	Value	Unit	Parameter	Value	Unit
C_0	0.0	Pa	A	609.77E9	Pa
C_1	0.0	Pa	B	12.95E9	Pa
C_2	0.0	Pa	R_1	4.50	–
C_3	0.0	Pa	R_2	1.40	–
C_4	0.4	–	ω	0.25	–
C_5	0.4	–	E_0	9.00E9	Pa
C_6	0.0	–			
E_0	253.40E3	Pa			

A 250×250 mm rectangular domain of 1 mm square axi-symmetric 2D-ALE elements was used for both spherical and cylindrical charge configurations. The y-axis represented the axis of symmetry, and the top edge of the domain was constrained against normal translations to act as a rigid boundary. The

two remaining domain edges (i.e. those remote from the charge) were set as non-reflecting boundaries to allow the blast wave to freely propagate out of the domain. A preliminary mesh sensitivity study indicated that a 1 mm mesh was adequate to achieve impulse convergence, and that an increase or decrease in the default bulk viscosity parameters had little effect on the fidelity or accuracy of the results.

Initially the domain was filled with air, and the `*INITIAL_VOLUME_FRACTION_GEOMETRY` keyword was used to ‘fill’ the explosive volume. For the spherical charge, container type 6 (sphere) was selected, and a 24.6 mm radius sphere – with its centre on the axis of symmetry and 80 mm from the reflecting boundary – was specified. For the cylindrical charge, container type 5 (rectangular box) was selected, with one corner located on the axis of symmetry, 168 mm from the reflecting boundary, and the other corner located 28.6 mm from the axis of symmetry and 187 mm from the reflecting boundary (Figure 2). Each shape would form a sphere and cylinder respectively when rotated about the y -axis.

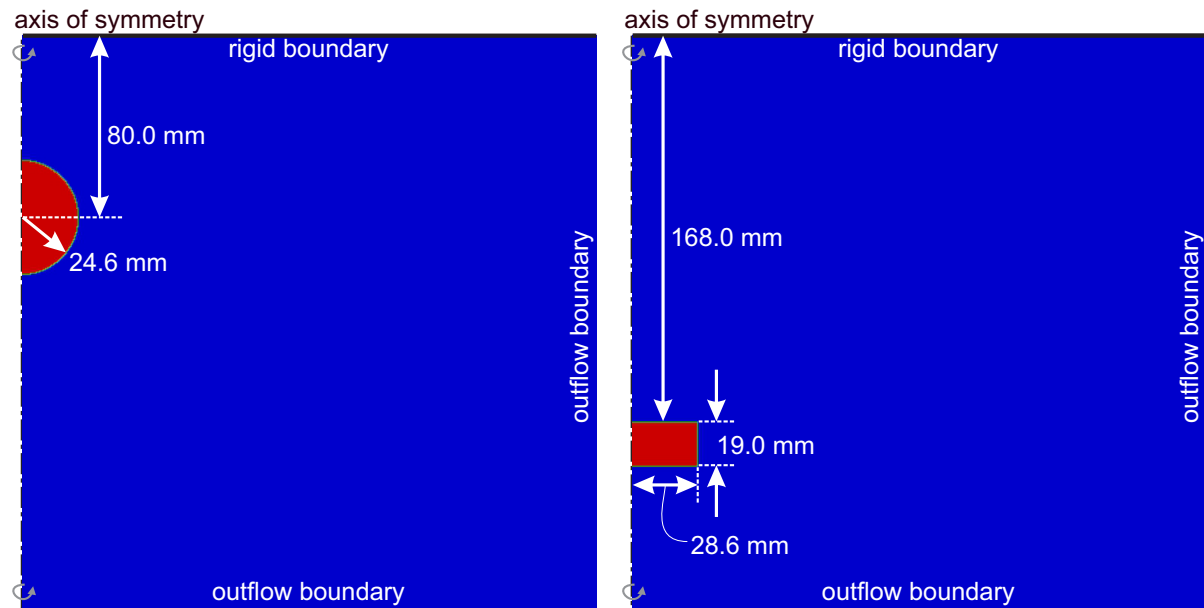


Figure 2: Geometry of the spherical [left] and cylindrical [right] charge models

4 Results

Figure 3 shows numerical and experimental¹ pressure–time and specific impulse–time histories following the detonation of a 100 g PE4 sphere at 55.4 mm clear stand-off from a rigid target. Figure 4 shows numerical and experimental pressure–time and specific impulse–time histories following the detonation of a 78 g PE4 3:1 cylinder at 168.0 mm clear stand-off. Numerical modelling results were output at locations slightly offset from the rigid target surface using the `*DATABASE_TRACER` keyword. Ambient pressure (101.36 kPa) was subtracted from the results to give values in terms of overpressure, and trapezoidal numerical integration was used to determine impulse histories from the data. Experimental results have been time-shifted back by 50 μ s to account for the time taken for each stress pulse to reach the gauge location from the face of the HPB.

Numerical and experimental peak specific impulse distributions, out to 100 mm from the target centre, are shown for spherical charges in Figure 5a), and for cylindrical charges in Figure 5b). There are twelve data points at each radial ordinate per charge configuration: four HPBs at each radial ordinate per test (see Figure 1b), with the exception of the centre of the plate where there are three data points per charge configuration as only one HPB was used per test.

¹Here, experimental results are shown for one representative HPB array in one of the 3 tests per charge configuration

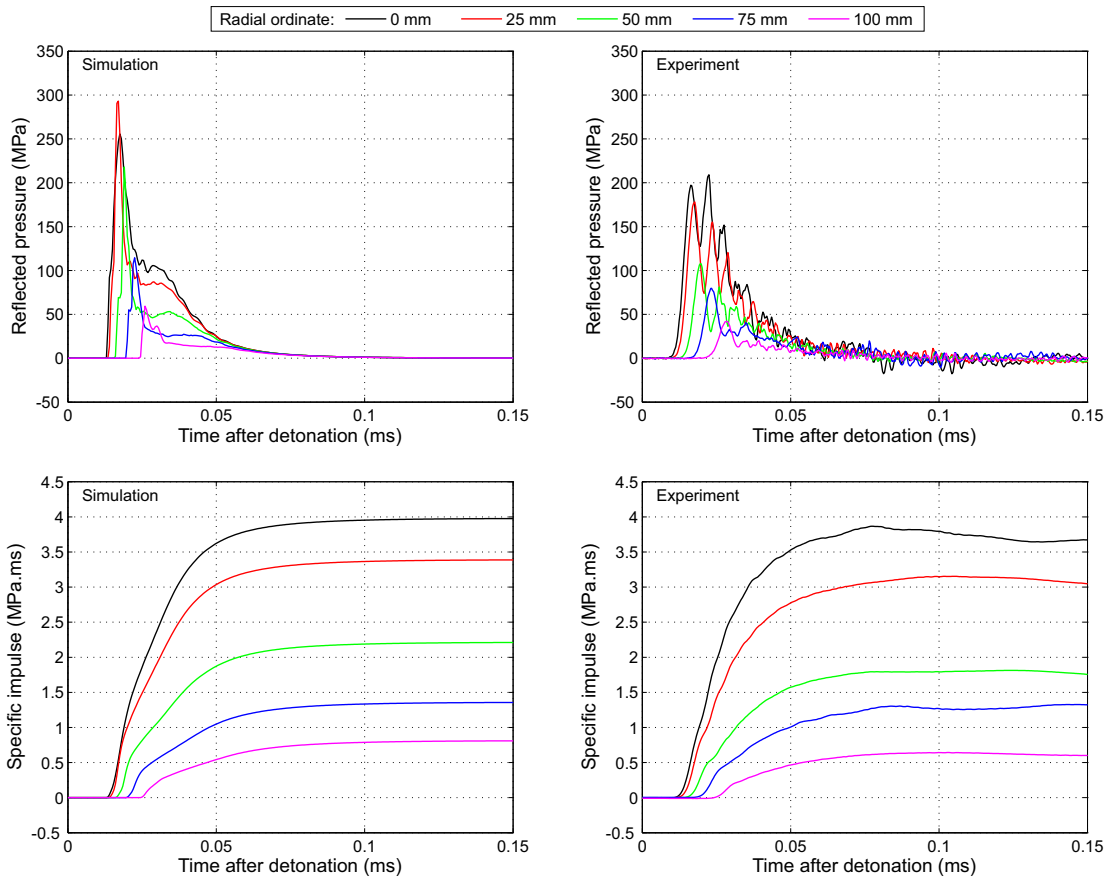


Figure 3: Numerical pressure–time and specific impulse–time histories (100 g PE4 sphere at 55.4 mm clear stand-off) compared with data from Test 1

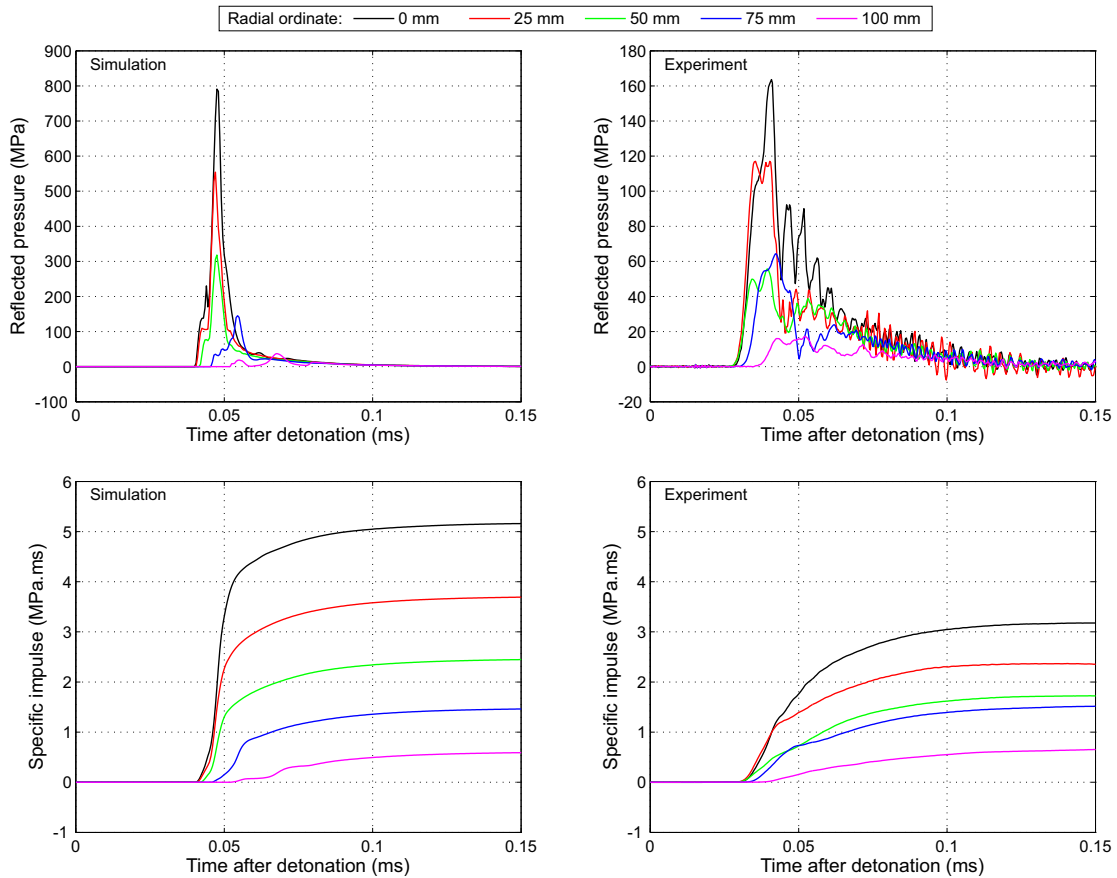


Figure 4: Numerical pressure–time and specific impulse–time histories (78 g PE4 3:1 cylinder at 168.0 mm clear stand-off) compared with data from Test 5

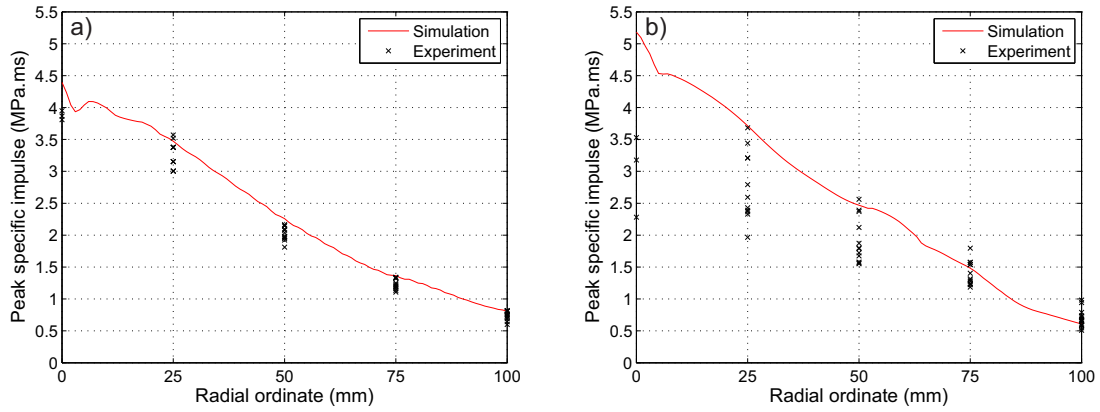


Figure 5: Numerical and experimental peak specific impulse distributions: a) 100 g sphere at 55.4 mm clear stand-off; b) 78 g 3:1 cylinder at 168.0 mm clear stand-off

5 Discussion

The numerical spherical pressure–time and impulse–time histories appear to be in good agreement with the experimental results (Figure 3). The experimental signals display some evidence of Pochhammer-Chree (PC) dispersion [13] in the form of a general ‘rounding’ of the pressure signal and the presence of spurious high frequency oscillations following the head of the pulse. Current PC dispersion correction methods are unable to correct the higher frequency components that are typically seen in blast pressure signals [14]. Despite this, pressure magnitudes and durations appear similar at all bar locations, and the numerical distribution of specific impulse (Figure 5a) follows the experimentally recorded specific impulses closely.

Conversely, the agreement between the numerical and experimental cylindrical pressure–time histories is comparatively poor, particularly for the central bar where the numerical peak pressure (~ 800 MPa) is approximately five times greater than the experimental value (~ 160 MPa). The numerical impulse–time histories demonstrate a less gradual rise to peak value, indicating a much sharper steeper decay during the positive phase duration when compared to the experimental recordings. Whilst some rounding and lengthening of the shock front is to be expected when using a HPB (owing to PC dispersion), such a disparity between simulated and recorded results suggests that there is a fundamental difference between the mechanisms driving blast load development in the model and experiment, particularly in the region directly above the charge.

The numerical cylindrical specific impulse is in better agreement with the experimental results at the 75 mm and 100 mm radial ordinates (Figure 5b). It is therefore likely that the total numerical impulse (i.e. the area under the specific impulse vs radial ordinate curve when rotated around the vertical axis) would more closely match the experimental value, owing to the greater area represented by the bars further from the plate centre and hence greater ‘weighting’ of the more accurate specific impulses. Accordingly, we might expect LS-DYNA to be able to simulate the deformation of, for example, a steel plate loaded by the blast from a near-field cylindrical explosive to a reasonable level of accuracy. However, it is clear from the above that the numerical model would not be fully representing the physics correctly.

Why then, are the spherical results in good agreement yet the cylindrical results are not? Figure 6 shows: [left] the dominant fluid material within each cell of the numerical model, with blue representing air and red representing the high explosive detonation products, and; [right] high speed video stills from a representative cylindrical test.

Qualitatively, the model and experiment appear in good agreement, with similar fireball expansion rates.² The fireball appears more ‘flat-topped’ in the model, with a more regular overall shape when compared to the mottled surface of the fireball in the experiment. It is not clear whether these differences are significant enough to cause the discrepancies between simulation and experiment seen in Figure 4, or whether the differences are caused by inaccuracies in the pressure–volume–energy state of the numerical

²The experiment can be seen to arrive marginally earlier, which is in agreement with arrival times in Figure 4.

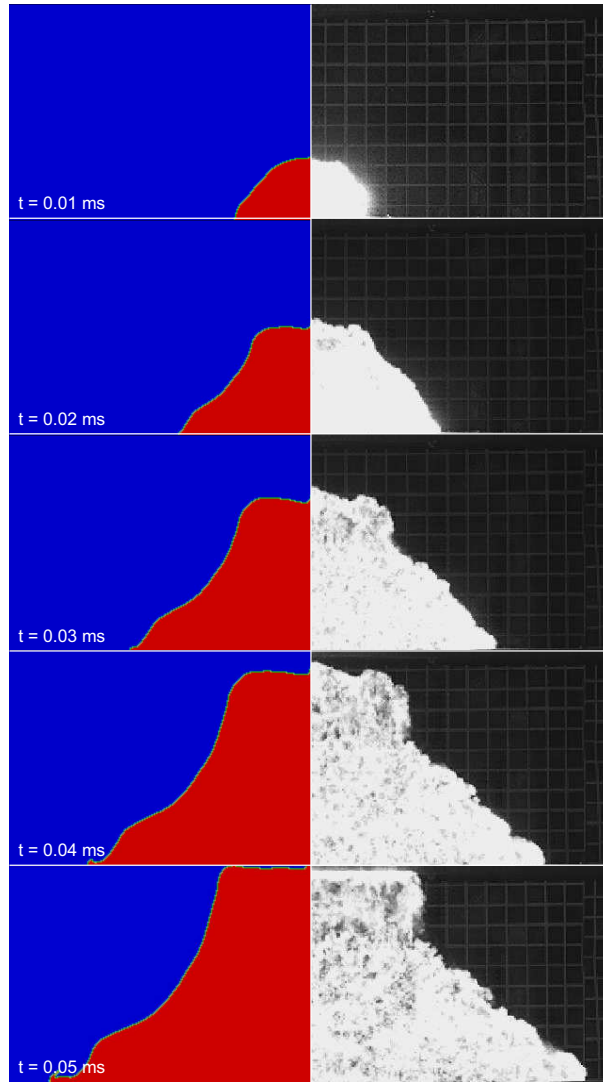


Figure 6: Numerical [left] and experimental [right] fireball expansion at 0.01 ms intervals

detonation products. The relatively good agreement attained by the spherical model, and the accuracy with which far-field blast events have been simulated in previous studies [15], suggests that the pressure–volume–energy relationship of the explosive is valid, and instead the inaccuracies seen herein are as a result of LS-DYNA’s inability to correctly simulate strongly directional shock waves, such as those caused by cylindrical charges. This issue is currently being investigated by researchers in the Blast and Impact Dynamics Group at the University of Sheffield.

6 Summary and conclusions

This paper presents the results from experimental test conducted at the University of Sheffield, UK. Two different charge configurations were tested: 100 g spheres detonated at 55.4 mm clear distance from a rigid target, and 78 g cylindrical (3:1 diameter:height) PE4 charges detonated 168.0 mm clear distance from a rigid target. The spatial and temporal distribution of pressure was directly measured using an array of 17 HPBs sat flush with the reflecting surface. LS-DYNA was used to simulate the blast events, and the results were compared against the experimental recordings. The spherical model was in good agreement with the experiments, however the agreement was considerably less good for the cylindrical charges. Despite the differences in the form and magnitude of the pressure signals, the fireball expansion rate and shape/volume was shown to be similar for the cylindrical charge simulation and experiments. This study presents valuable validation data and indicates that, whilst LS-DYNA is suitable for simulating near-field spherical charges, it may not be suitable for situations involving strongly

directional shocks. Furthermore, this paper highlights the need for both qualitative and quantitative validation data: validating numerical models with qualitative data alone, or data that ‘smears’ results over a larger area (i.e. total spatially integrated impulse) may be misleading. It is only with detailed quantitative data that we can begin to unpick some of the physical mechanisms associated with near-field blast loading.

References

- [1] E. Esparza. Blast measurements and equivalency for spherical charges at small scaled distances. *International Journal of Impact Engineering*, 4(1):23–40, 1986.
- [2] C. N. Kingery and G. Bulmash. Airblast parameters from TNT spherical air burst and hemispherical surface burst. Technical Report ARBRL-TR-02555, U.S Army BRL, Aberdeen Proving Ground, MD, USA, 1984.
- [3] S.E. Rigby, A. Tyas, S. D. Fay, S. D. Clarke, and J. A. Warren. Validation of semi-empirical blast pressure predictions for far field explosions – is there inherent variability in blast wave parameters? In *6th International Conference on Protection of Structures Against Hazards (PSH14)*, Tianjin, China, 2014.
- [4] J. Shin, A. S. Whittaker, and D. Cormie. Incident and normally reflected overpressure and impulse for detonations of spherical high explosives in free air. *Journal of Structural Engineering*, 04015057(13):1–13, 2015.
- [5] J. O. Hallquist. *LS-DYNA Theory Manual*. Livermore Software Technology Corporation, CA, USA, 2006.
- [6] S. D. Clarke, S. D. Fay, J. A. Warren, A. Tyas, S. E. Rigby, and I. Elgy. A large scale experimental approach to the measurement of spatially and temporally localised loading from the detonation of shallow-buried explosives. *Measurement Science and Technology*, 26:015001, 2015.
- [7] B. Hopkinson. A method of measuring the pressure produced in the detonation of high explosives or by the impact of bullets. *Philosophical Transactions of the Royal Society of London. Series A, Containing Papers of a Mathematical or Physical Character*, 213(1914):437–456, 1914.
- [8] S.E. Rigby, S.D. Fay, S.D. Clarke, A. Tyas, J.J. Reay, J.A. Warren, M. Gant, and I. Elgy. Measuring spatial pressure distribution from explosives buried in dry leighton buzzard sand. *International Journal of Impact Engineering*, 96:89–104, 2016.
- [9] S. E. Rigby, A. Tyas, R. J. Curry, and G. S. Langdon. Experimental measurement of specific impulse distribution and transient deformation of plates subjected to near-field explosive blasts. *Submitted for possible publication in International Journal of Impact Engineering*.
- [10] E. L. Lee, H. C. Hornig, and J. W. Kury. Adiabatic expansion of high explosive detonation products. Technical Report TID 4500-UCRL 50422, Lawrence Radiation Laboratory, University of California, CA, USA, 1968.
- [11] D. Bogosian, M. Yokota, and S. Rigby. TNT equivalence of C-4 and PE4: A review of traditional sources and recent data. In *Proceedings of the 24th International Symposium on Military Aspects of Blast and Shock (MABS24)*, Halifax, Nova Scotia, Canada, 2016.
- [12] B. M. Dobratz and P. C. Crawford. LLNL explosives handbook – properties of chemical explosives and explosive simulants. Technical Report UCRL 52997, Lawrence Livermore National Laboratory, University of California, CA, USA, 1985.
- [13] D. Bancroft. The velocity of longitudinal waves in cylindrical bars. *Physical Review*, 59:588–593, 1941.
- [14] S. E. Rigby, A. D. Barr, and M. Clayton. A review of Pochhammer-Chree dispersion in the Hopkinson bar. doi:10.1680/jencm.16.00027, 2018.
- [15] S. E. Rigby, A. Tyas, T. Bennett, S. D. Fay, S. D. Clarke, and J. A. Warren. A numerical investigation of blast loading and clearing on small targets. *International Journal of Protective Structures*, 5(3):253–274, 2014.